J Mater Sci (2008) 43:2072–2076
DOI 10.1007/s10853-007-2442-8

LETTER

Large magnetoelectric coefficient in Co-fired Pb $(Zr_{0.52}Ti_{0.48})O_3$–Pb $(Zn_{1/3}Nb_{2/3})O_3$–$Ni_{0.6}Cu_{0.2}Zn_{0.2}Fe_2O_4$ trilayer magnetoelectric composites

Rashed Adnan Islam · Shashank Priya

Received: 21 December 2007 / Accepted: 28 December 2007 / Published online: 17 January 2008

Introduction

Magnetoelectric materials possess coupling between the ferroic properties polarization, and magnetization [1–4]. The interrelation between ferroelectricity and magnetization allows the magnetic control of ferroelectric properties and vice versa. Single phase magnetoelectric (ME) materials (such as Cr_2O_3, $BiFeO_3$, $YMnO_3$, etc.) suffer from the drawback that ME effect is weak [5–7]. Better alternatives are ME composites that have higher magnitudes of the ME voltage coefficient exploiting the product property of the materials [8–10]. Magnetoelectric (ME) effect in a particulate sintered composite was obtained by combining magnetostrictive and piezoelectric phases [11–15]. Sintered composites have many advantages, such as simplicity in synthesis, cost-effective materials and fabrication process, and better control of desired geometry. However, the ME response is low of the order of 100 mV/cm Oe. Recently, laminated magnetoelectric (ME) composites synthesized by using giant piezoelectric and magnetostrictive materials have gained attention because they exhibit superior ME response [16–19]. Dong et al. [20] have reported a composite where piezofiber is laminated between the high permeability magnetostrictive FeBSiC alloy using epoxy and found a large response of 22 V/cm Oe at 1 Hz.

The research on sintered composites has shown that corfiring multiple layers can provide higher ME coefficients. However, the drawback is that tape-casting process for synthesizing multilayers of heterogeneous materials is complex. Further, in order to improve the property of the sintered ME composites, the other variables such as composition, microstructure, geometry, texture, and post sinter heat treatment needs to be optimized. In our previous studies, it has been shown that soft piezoelectric phase (high dielectric and piezoelectric constant), soft magnetic phase (high permeability and low coercivity) [21], large piezoelectric grain size (>1 μm) [22], layered structure (bilayer/trilayer) [23] and post-sintering thermal treatment (annealing and aging) [24] improve the magnetoelectric property. In order to combine all the parameters together, the challenge is to develop a unique fabrication process, in which layers of piezoelectric and magnetostrictive can be cofired together. Moreover the poling process of the piezoelectric phase requires high resistivity, and thus electrodes have to be preserved during sintering.

We found that pressure assisted sintering can produce trilayer composites with any desired dimensions. Further, we designed the compositions such that sintering could be done at low temperatures of 900 °C which results in stable electrodes. The objective of this letter is to analyze the microstructural, piezoelectric, dielectric, and magnetoelectric properties of this trilayer sintered ME composite.

Experimental

Powders of 0.9 Pb $(Zr_{0.52}Ti_{0.48})O_3$–0.1 Pb $(Zn_{1/3}Nb_{2/3})O_3$ [0.9 PZT–0.1 PZN] and $Ni_{0.6}Cu_{0.2}Zn_{0.2}Fe_2O_4$ [NCZF] were synthesized using conventional mixed oxide method. In order to fabricate a trilayer sample, at first a layer of

R. A. Islam
Materials Science and Engineering, University of Texas at Arlington, Arlington, TX 76019, USA

S. Priya (✉)
Materials Science and Engineering, Virginia Tech, Blacksburg, VA 24061, USA
e-mail: spriya@vt.edu

NCZF powder (no binder was used) was pressed uniaxially at 5 MPa pressure inside a hardened steel die of diameter 12.5 mm and then Ag–Pd (DuPont 6160 conductor paste) electrode was printed. The second layer of 0.9 PZT–0.1 PZN was pressed on top of Ag–Pd under 5 MPa pressure inside the same die and then the electrode was applied again. The third and the final layer of NCZF layer was pressed on top of second electrode layer. The five-layer structure NCZF/Ag–Pd/PZT–PZN/Ag–Pd/NCZF was then pressed under 20 MPa followed by cold isostatic press (CIP) under 207 MPa.

Figure 1a shows the schematic representation of trilayer sample where piezoelectric phase is sandwiched between magnetostrictive phases. The pressed pellet was dried at 100 °C for 10 min and then placed inside a Lyndberg BlueM furnace according to the set up shown in Fig. 1b. The sintering was done at 900 °C under a pressure of 30 kPa with very slow heating and cooling rate (∼1°C/min). Figure 1c shows the sintered trilayer sample with dimensions of 3.25 mm in thickness and 11 mm in diameter. Annealing was done after sintering at 800 °C for 10 h under load. In order to polarize the samples, Ag–Pd electrode (DuPont 7714 conductor paste) was applied on top and bottom of the sample. The top electrode layer of the composite was then connected to the top of the PZT as shown in Fig. 1a, b. Similarly, bottom electrode of the composite was connected to the bottom electrode of the PZT using same Ag–Pd electrode. The poling was done at 110 °C for 20 min under 2.2 kV/mm electric field. Microstructural analysis of the sintered samples was done by a Zeiss Leo Smart SEM using polished and thermally etched samples. Dielectric constant measurements were performed using a HP 4284 LCR meter; and the ME voltage coefficient by a lock-in amplifier method.

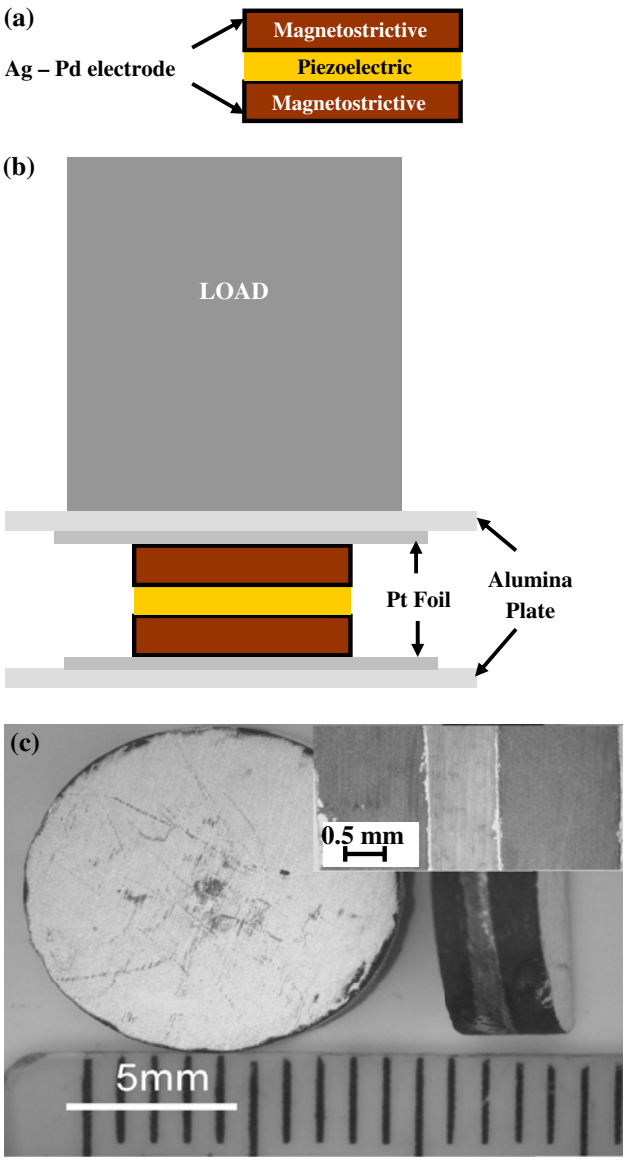

Fig. 1 (**a**) Schematic representation of the trilayer composites, (**b**) schematic diagram of sintering set up and (**c**) optical image of sintered sample (inset—cross-section)

Results and discussion

Figure 2a shows the low magnification SEM image of the sintered sample. The interface electrode layers are 10 μm thick; center layer is 0.9 PZT–0.1 PZN, whereas outside layers are NCZF. There were some micro and macrocracks formed during the sintering which could be related to the thermal mismatch between these three layers and insufficient homogenization. Figure 2b shows the magnified view of the interface. The microstructure is dense in both the phases with excellent adherence with the Ag–Pd electrode. Figure 2c and d shows the low magnification image and interface microstructure of the annealed samples. The annealing treatment resulted in the homogenization at the interface reducing the porosity and microcrack density. The macrocracks were still present in the structure. Figure 2e, f shows the high magnification grain structure of the sintered 0.9 PZT–0.1 PZN and NCZF. The grain size observed in 0.9 PZT–0.1 PZN was more than 1 μm and that in NCZF in the range of 3–5 μm.

Table 1 compares the piezoelectric and dielectric properties of sintered and annealed samples. A significant increase in piezoelectric and dielectric properties was observed after annealing which is consistent with our previous results. The magnitude of the electromechanical coefficients d_{33}, g_{33}, $\varepsilon_r/\varepsilon_o$ increased from 204 pC/N, 20.4 × 10^{-3} Vm/N, and 1,132 to 250 pC/N, 22.4 × 10^{-3} Vm/N, and 1,257. The magnitude of the loss factor (tan δ) decreased from 5.08% to 3.45% at room temperature. The loss factor increased sharply at high temperature which could be related to space charge polarization. At 100 kHz, the Curie temperature observed was

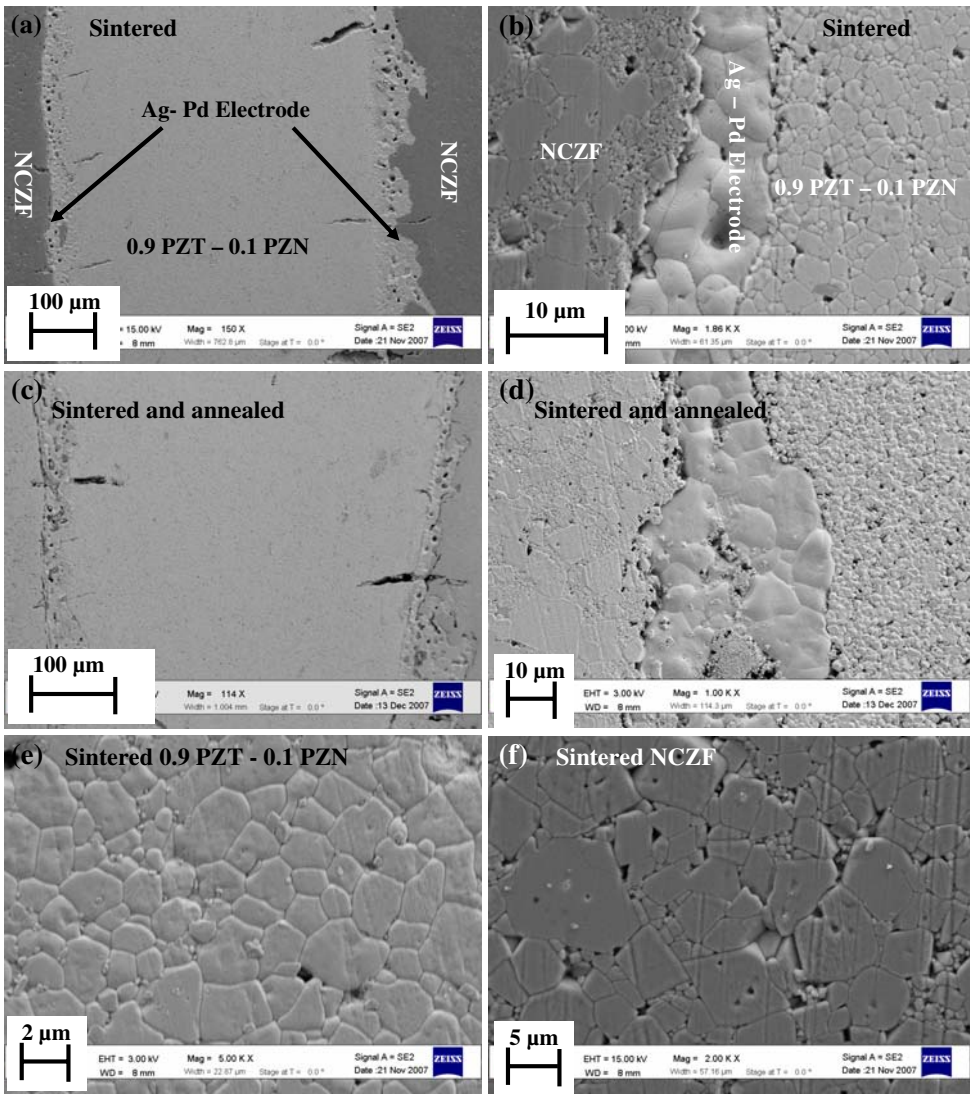

Fig. 2 SEM micrographs. (**a**) Low magnification image of sintered trilayer sample, (**b**) interface microstructure, (**c**) low magnification image of sintered and annealed sample, (**d**) interface microstructure of sintered and annealed trilayer sample, (**e**) grain structure of PZT side and (**f**) grain structure of NZF side

Table 1 Piezoelectric properties of NCZF–(0.9 PZT–0.1 PZN)–NCZF trilayer after different thermal treatment

	Sintered	Sintered and annealed
Piezoelectric constant, d_{33}	204 pC/N	250 pC/N
Dielectric constant, $\varepsilon_r/\varepsilon_o$ (at 1 kHz)	1,132	1,257
Dielectric loss, tan δ (at 1 kHz)	5.08%	3.45%
Piezoelectric voltage constant, g_{33}	20.4×10^{-3} Vm/N	22.46×10^{-3} Vm/N
Coupling coefficient, k_p	0.14%	0.1638%
Resonance frequency, f_s	258 kHz	255 kHz
Antiresonance frequency, f_a	261 kHz	258 kHz

around 330 °C. Figure 3 shows the resonance spectrum of the sintered and annealed samples. Interestingly, the spectrum for annealed sample has less spurious and lower impedance at the resonance indicating high mechanical quality factor.

Figure 4 shows the magnetoelectric behavior of trilayer composite. The magnitude of the ME coefficient for sintered sample was of the order of 412 mV/cm Oe with saturation field near 400 Oe. Annealed samples showed improved ME coefficient of 494 mV/cm Oe about 20% higher than sintered ones. This magnitude is quite high from that previously reported for sintered composites. Srinivasan et al. [25] have derived the transverse ME coefficient for the layered composite as following:

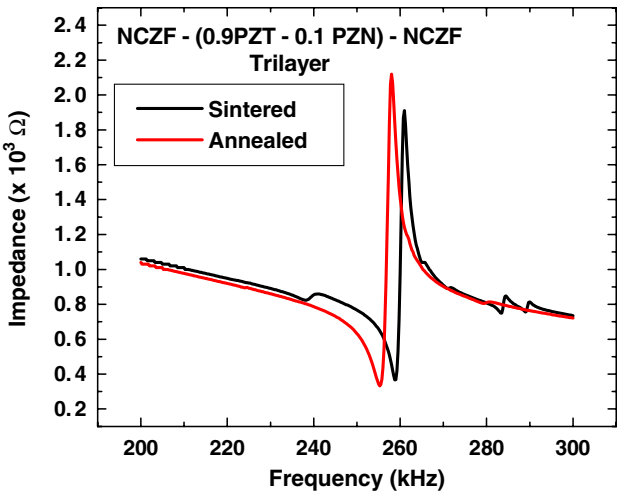

Fig. 3 Impedance spectrum of the trilayer composite

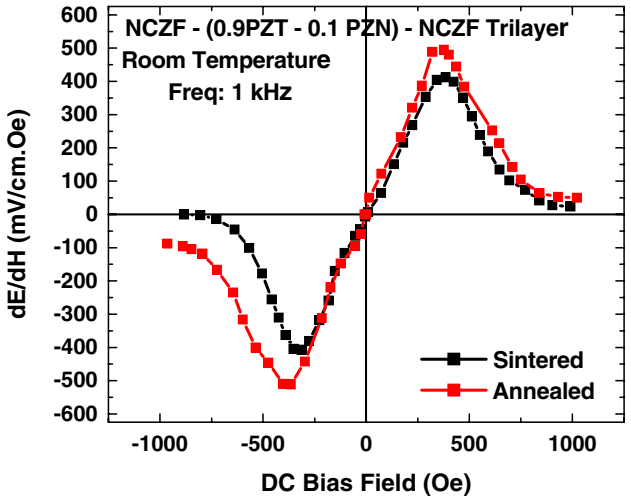

Fig. 4 Magnetoelectric coefficient as a function of dc bias field

$$\frac{\delta E_3}{\delta H_1} = \frac{-2d_{31}^{p} q_{11}^{m} v^{m}}{(s_{11}^{m} + s_{12}^{m})\varepsilon_{33}^{T,P} v^{p} + (s_{11}^{p} + s_{12}^{p})\varepsilon_{33}^{T,P} v^{m} - 2(d_{31}^{p})^2 v^{m}} \quad (1)$$

$$\frac{\delta E_3}{\delta H_1} = \frac{-2d_{31}^{p} q_{11}^{m} \frac{t_m}{t_m+t_p}}{(s_{11}^{m} + s_{12}^{m})\varepsilon_{33}^{T,P} \frac{t_p}{t_m+t_p} + (s_{11}^{p} + s_{12}^{p})\varepsilon_{33}^{T,P} \frac{t_m}{t_m+t_p} - 2(d_{31}^{p})^2 \frac{t_m}{t_m+t_m}} \quad (2)$$

where d_{31}^{p} is the piezoelectric coefficient, v^{m} and v^{p} are the volume of magnetic and piezoelectric phase, t_m and t_p are the thickness of magnetic and piezoelectric phase, s_{11}^{p}, s_{12}^{p} are the elastic compliances for piezoelectric phase, s_{11}^{m}, s_{12}^{m} are the elastic compliances for magnetostrictive phase, q_{11} is the piezomagnetic coefficient of the magnetic phase and $\varepsilon_{33}^{T,P}$ is the permittivity of the piezoelectric phase. For a radial mode disk, s_{11}^{p} can be calculated as following:

$$s_{11}^{p} = \frac{\eta_1^2}{\rho(2\,\pi\, f_s a)^2[1-(\sigma^{p})^2]} \quad (3)$$

where η_1 is the frequency constant, σ^{p} is the planar Poison's ratio, f_s is the resonance frequency, a is the radius and ρ is the density ($\sim$7.52 g/cc). The coefficients η_1 and σ^{p} can be found by measuring ratio of first overtone ($\sim$670 kHz for sintered samples) to fundamental resonance frequency (258 kHz) [26]. For the ratio of 2.602, η_1 and σ^{p} values were found to be 2.074 and 0.341, respectively, from IEEE standards. Using these values s_{11}^{p} can be calculated as 8.66×10^{-12} m^2/N. The transverse mode coupling constant k_{31} can be calculated by using the following expression [26]:

$$k_{31}^2 = k_p^2 \frac{(1-\sigma_p)}{2} \quad (4)$$

The values of planar coupling constant k_p are listed in Table 1. Using these values the magnitude of k_{31} is found to be 0.0803%. If k_{31} and s_{11}^{E} are known, then d_{31} can be calculated as following

$$k_{31}^2 = \frac{d_{31}^2}{(s_{11}^{E}\varepsilon_{33}^{T})} \quad (5)$$

The magnitude of d_{31} was found to be as 23.66×10^{-12} C/N. The magnitude of s_{12}^{E} was found to be—2.96×10^{-12} m^2/N using the following expression [27]:

$$k_p^2 = \frac{2d_{31}^2}{[(s_{11}^{E} + s_{12}^{E})\varepsilon_{33}^{T}]} \quad (6)$$

Using the values of s_{11}^{m}, s_{12}^{m} as 6.5×10^{-12} m^2/N and -2.4×10^{-12} m^2/N [25], q_{11} as -65×10^{-9} Oe (at 400 Oe field), $\frac{t_m}{t_m+t_p}$ and $\frac{t_p}{t_m+t_p}$ as 0.7 and 0.3, respectively, the magnitude of the ME coefficient computed from Eq. 2 was found to be 437.1 mV/cm Oe. This calculated value is close to the experimentally measured value of 412 mV/cm Oe. The calculated magnitude of the ME coefficient for the annealed samples was of the order of 468 mV/cm Oe.

Conclusion

In summary, NCZF–(0.9 PZT–0.1 PZN)–NCZF trilayer was fabricated using pressure assisted sintering. In the sintered sample, piezoelectric phase had grain size of more than 1 μm, while magnetostrictive phase had grain size of 3–5 μm. Sintered and annealed samples showed ME coefficient of $\sim$494 mV/cm Oe, which is quite large compared to the previously reported values for particulate sintered composites. This magnitude can be further

enhanced by reducing the macrodefects and optimization of ferrite to PZT thickness.

Acknowledgement The authors gratefully acknowledge the support from Army Research Office and Department of Energy.

References

1. Wang J, Zheng H, Lofland SE, Ma Z, Ardabili LM, Zhao T, Riba LS, Shinde SR, Ogale SB, Bai F, Viehland D, Jia Y, Schlom DG, Wuttig M, Roytburd A, Ramesh R (2004) Science 303:661
2. Ederer C, Spaldin N (2004) Nat Mater 3:849
3. Eerenstein W, Mathur ND, Scott JF (2006) Nature 442:759
4. Hur N, Park S, Sharma PA, Ahn JS, Guha S, Cheong SW (2004) Nature 429:392
5. Astrov DN (1960) Sov Phys JETP 11:708
6. Wang J, Neaton JB, Zheng H, Nagarajan V, Ogale SB, Liu B, Viehland D, Vathiyanathan V, Schlom DG, Waghmare UV, Spaldin NA, Rabe KM, Wuttig M, Ramesh R (2003) Science 299:1719
7. Van Aken BB, Palstra TTA, Filippetti A, Spaldin NA (2004) Nat Mater 3:164
8. Zheng M, Wan JG, Wang Y, Yu H, Liu JM, Jiang XP, Nan CW (2004) J Appl Phys 95(12):8069
9. Ryu J, Carazo AV, Uchino K, Kim H (2001) J Electoceram 7:17
10. Flores VC, Baques DB, Flores DC, Aquino JAM (2006) J Appl Phys 99:08J503
11. Van Suchetelene J (1972) Philips Res Rep 27:28
12. Weng L, Fu Y, Song S, Tang J, Li J (2007) Scripta Mater 56:465
13. Ren SQ, Weng LQ, Song SH, Li F, Wan JG, Zeng M (2005) J Mater Sci 40(16):4375. doi:10.1007/s10853-005-1057-1
14. Wu D, Gong W, Deng H, Li M (2007) J Phys D: Appl Phys 40:5002
15. Srinivasan G, DeVreugd CP, Flattery CS, Laletsin VM, Paddubnaya N (2004) Appl Phys Lett 85(13):2550
16. Ryu J, Priya S, Uchino K, Viehland D, Kim H (2002) J Korean Ceram Soc 39:813
17. Ryu J, Priya S, Uchino K, Kim H (2002) J Electroceram 8:107
18. Srinivasan G, Rasmussen E, Levin B, Hayes R (2002) Phys Rev B 65:134402
19. Dong SX, Zhai J, Li JF, Viehland D (2006) J Appl Phys 88:082907
20. Dong S, Zhai J, Li JF, Viehland D (2006) Appl Phys Lett 89:252904
21. Islam RA, Viehland D, Priya S (2008) J Mater Sci Lett 43(4):1497
22. Islam RA, Priya S (2007) J Mater Sci (submitted)
23. Islam RA, Priya S (2006) J Appl Phys Lett 89:152911
24. Islam RA, Jiang JC, Priya S, Bai F, Viehland D (2007) Appl Phys Lett 91:162905
25. Srinivasan G, Rasmussen E, Gallegos J, Srinivasan R, Bokhan YI, Laletin VM (2001) Phys Rev B 64:214408
26. American National Standard Institute (1987) IEEE Standard on Piezoelectricity
27. APC International (2002) Piezoelectric ceramics: principle and applications, ISBN 0-9718744-0-9